Physics Letters B 783 (2018) 263–267

Contents lists available at ScienceDirect

Physics Letters B

www.elsevier.com/locate/physletb

Parton distribution amplitudes: Revealing correlations within the proton and Roper

Cédric Mezrag [a,b,*], Jorge Segovia [c,*], Lei Chang [d,*], Craig D. Roberts [b,*]

[a] Istituto Nazionale di Fisica Nucleare, Sezione di Roma, P. le A. Moro 2, I-00185 Roma, Italy
[b] Physics Division, Argonne National Laboratory, Argonne, IL 60439, USA
[c] Institut de Física d'Altes Energies (IFAE) and Barcelona Institute of Science and Technology (BIST), Universitat Autònoma de Barcelona, E-08193 Bellaterra, Barcelona, Spain
[d] School of Physics, Nankai University, Tianjin 300071, China

ARTICLE INFO

Article history:
Received 23 February 2018
Received in revised form 12 June 2018
Accepted 28 June 2018
Available online 2 July 2018
Editor: J.-P. Blaizot

Keywords:
Parton distribution amplitudes
Proton structure
Nonperturbative methods in quantum field theory
Dynamical chiral symmetry breaking
Light-front quantum field theory

ABSTRACT

Constrained by solutions of the continuum three-valence-body bound-state equations, we use perturbation theory integral representations (PTIRs) to develop algebraic *Ansätze* for the Faddeev wave functions of the proton and its first radial excitation, delivering therewith a quantum field theory calculation of the pointwise behaviour of their leading-twist parton distribution amplitudes (PDAs). The proton's PDA is a broad, concave function, with its maximum shifted relative to the peak in QCD's conformal limit expression for this PDA. The size and direction of this shift signal the presence of *both* scalar and pseudovector diquark correlations in the nucleon, with the scalar generating around 60% of the proton's normalisation. The radial-excitation is constituted similarly, and the pointwise form of its PDA, which is negative on a material domain, is the result of marked interferences between the contributions from both types of diquark; particularly, the locus of zeros that highlights its character as a radial excitation. These features originate with the emergent phenomenon of dynamical chiral-symmetry breaking in the Standard Model.

1. Introduction

Wave functions provide insights into composite systems, *e.g.* they express the presence and extent of correlations between constituents, and their signature in scattering processes; and thereby bridge experiment and theory. This is true within quantum chromodynamics (QCD), but there are difficulties. Everyday hadrons (p = proton, neutron, *etc.*) are constituted from up (u) and down (d) valence-quarks; but the Higgs boson generates current-masses for these fermions which are more than 100-times smaller than the scale associated with the composite systems: $m_{u,d} \approx 2$–4 MeV cf. $m_p \approx 1$ GeV. Plainly, the interaction energy greatly exceeds the rest masses of the anticipated constituents, making inapplicable the wave functions typical of Schrödinger quantum mechanics.

The difficulties appear chiefly because particle-number is not conserved by boosts; and severe challenges are faced when constituents are light, *e.g.* wave functions describing incoming and outgoing scattering states then represent systems with different particle content, so a probability interpretation is lost. Such problems are circumvented by using a light-front formulation because eigenfunctions of the Hamiltonian are then independent of the system's four-momentum [1,2].

The light-front wave function of a hadron with momentum P and spin λ, $\Phi(P,\lambda)$, is complicated. In terms of perturbation theory's partons, $\Phi(P,\lambda)$ has a countably-infinite Fock-space expansion. Were it necessary to use this complete object in analyses of even the simplest processes, then little connection between experiment and theory could be made. Fortunately, collinear factorisation in the treatment of hard exclusive processes entails that much can be gained merely by studying hadron leading-twist parton distribution amplitudes (PDAs) [3]. Such a PDA is obtained from the simplest term in the Fock-space expansion.

Regarding S-wave ground-state light-meson leading-twist PDAs, the last decade has seen real progress, not concerning their conformal limit [3]: $\varphi(x;\zeta) = 6x(1-x)$, $m_{\rm p}/\zeta \simeq 0$; but on $m_p/\zeta \simeq 1$, where they are now known to be broad, concave functions [4–12]. This resolves a longtime conflict, removing the possibility that such PDAs have a minimum at zero relative momentum [13].

* Corresponding authors.
E-mail address: cdroberts@anl.gov (C.D. Roberts).

https://doi.org/10.1016/j.physletb.2018.06.062

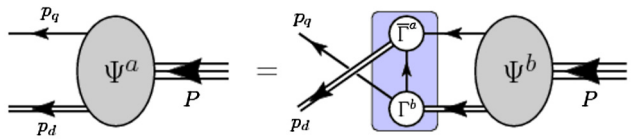

Fig. 1. Poincaré covariant Faddeev equation. The shaded rectangle demarcates its kernel: *single line*, dressed-quark propagator; Γ, diquark correlation amplitude; and *double line*, diquark propagator. Ψ is the Faddeev amplitude for a baryon of total momentum $P = (p_1 + p_2) + p_3 = p_d + p_q$. The wave function, χ, is obtained by attaching the quark and diquark propagator legs to Ψ.

Concerning the proton's leading-twist PDA, however, the situation is as unsatisfactory today as it was previously for mesons. Estimates of low-order Mellin moments exist, obtained using sum rules [13,14] or lattice-QCD (lQCD) [15–17], but there are no quantum field theory computations of this PDA's pointwise behaviour; and nothing is known about the PDA of the proton's radial excitation.

2. Proton PDA: definition

In the isospin-symmetry limit, the proton possesses one independent leading-twist (twist-three) PDA [18], denoted $\varphi([x];\zeta)$ herein:

$$\begin{aligned}&\langle 0|\varepsilon^{abc}\,\tilde{u}^a_+(z_1)\,C^\dagger \not{n}\, u^b_-(z_2)\not{n}\, d^c_+(z_3)|P,+\rangle\\ &=: \tfrac{1}{2} i f_p\, n\cdot P \not{n} N_+ \int_0^1 [dx]\,\varphi([x];\zeta) \mathrm{e}^{-in\cdot P\sum_i x_i z_i}, \end{aligned} \tag{1}$$

where $n^2 = 0$; (a,b,c) are colour indices; $q_\pm = H_\pm q := (1/2)(\mathbf{I}_{\mathrm{D}} \pm \gamma_5)q$, $\not{n} = \gamma\cdot n$; $\tilde{q}$ indicates matrix transpose; C is the charge conjugation matrix, $N = N(P)$ is the proton's Euclidean Dirac spinor; $\int_0^1 [dx] f([x]) = \int_0^1 dx_1 dx_2 dx_3 \delta(1-\sum_i x_i) f([x])$; and f_p measures the proton's "wave function at the origin".

$\varphi([x])$ can be computed once the proton's Poincaré-covariant wave function is in hand, *viz.*

$$\begin{aligned}&\langle 0|\epsilon^{abc}\tilde{u}^a(y_1)u^b(y_2)d^c(y_3)|P,\lambda\rangle =\\ &\int \prod_{i=1}^3 \left(\frac{\mathrm{d}^4 p_i}{(2\pi)^4} e^{-ip_i y_i}\right) \delta(P-\textstyle\sum_{i=1}^3 p_i)\,\chi(p_1,p_2,p_3,P)\,. \end{aligned} \tag{2}$$

Following thirty years of study [19–23], a clear picture has appeared. At an hadronic scale, the proton is a Borromean system, bound by two effects [24]: one originates in non-Abelian facets of QCD, expressed in the effective charge [25] and generating confined, nonpointlike but strongly-correlated colour-antitriplet diquarks in both the isoscalar-scalar and isotriplet-pseudovector channels; and that attraction is magnified by quark exchange associated with diquark breakup and reformation. The presence and character of the diquarks owe to the mechanism that dynamically breaks chiral symmetry in the Standard Model [24]. This understanding transforms the proton bound-state problem into that of solving the linear, homogeneous matrix equation in Fig. 1, which has been studied extensively, *e.g.* Refs. [24,26–31], so that the character of the solution is well known.

Recapitulating only essential features of the Faddeev equation solution herein, because extensive discussions are presented elsewhere, *e.g.* the appendices of Ref. [26], we recall that the proton Faddeev amplitude in Fig. 1 can be written:

$$\Psi(P) = \psi_1 + \psi_2 + \psi_3\,, \tag{3}$$

where the subscript identifies the bystander quark, *i.e.* the quark not participating in a diquark, ψ_3 gives $\psi_{1,2}$ by cyclic permutation of all quark labels, and

$$\psi_3(\{p\},\{\alpha\},\{\sigma\}) = \mathcal{N}_3^0 + \mathcal{N}_3^1, \tag{4a}$$

$$\mathcal{N}_3^0 = \left[\Gamma^0(k;K)\right]^{\alpha_1\alpha_2}_{\sigma_1\sigma_2} \Delta^0(K) \left[\mathcal{S}(\ell;P) N(P)\right]^{\alpha_3}_{\sigma_3}, \tag{4b}$$

$$\mathcal{N}_3^1 = \left[\Gamma^{1j}_\mu(k;K)\right]^{\alpha_1\alpha_2}_{\sigma_1\sigma_2} \Delta^1_{\mu\nu}(K) \left[\mathcal{A}^j_\nu(\ell;P) N(P)\right]^{\alpha_3}_{\sigma_3}, \tag{4c}$$

$(\{p\},\{\alpha\},\{\sigma\})$ are the momentum, isospin and spin labels of the dressed-quarks constituting the bound state; $P = p_1 + p_2 + p_3$ is the total momentum of the baryon; $k = p_1$, $K = p_1 + p_2$, $\ell = -K + (2/3)P$; and the j sum runs over the $(1,1) = +1$ and $(1,0) = 0$ isospin projections. The matrix-valued functions Γ in Eqs. (4) are the diquark correlation amplitudes in Fig. 1; Δ^0, $\Delta^1_{\mu\nu}$ are the associated dressed-propagators; and $\mathcal{S}$, $\mathcal{A}^j_\mu$ are matrix-valued quark–diquark amplitudes, describing the relative-momentum correlation between the diquark and bystander quark, *viz.* they are the objects returned by solving the Faddeev equation.

The proton's Faddeev wave function, χ, is obtained from Eqs. (3), (4) by attaching the appropriate dressed-quark and -diquark propagators. All relevant quantities are known and we therefore proceed by using algebraic representations for every element, with each form and their relative strengths, when combined, based on the results of modern analyses [24,26–31]. The dressed-quark and -diquark propagators are:

$$S(p) = (-i\not{p} + M)\sigma_M(p^2)\,,\ \sigma_M(s) = 1/[s+M^2]\,, \tag{5a}$$

$$\Delta^0(K) = \sigma_{M_0}(K^2)\,,\ \Delta^1_{\mu\nu}(K) = T_{\mu\nu}(K)\sigma_{M_1}(K^2)\,, \tag{5b}$$

$\hat{\sigma}_M(s) = M^2\sigma_M(s)$; $T_{\mu\nu}(K) = [\delta_{\mu\nu} - K_\mu K_\nu/K^2]$;

$$n_0\Gamma^0(k;K)C^\dagger = i\gamma_5 \int_{-1}^1 dz\,\rho(z)\,\hat{\sigma}_{\Lambda_\Gamma}(k^2_{+K})\,, \tag{6a}$$

$$\begin{aligned} n_1\Gamma^1_\mu(k;K)C^\dagger &= i(\gamma^{\mathrm{T}}_\mu + r_1 f(k;K)[\not{k},\gamma^{\mathrm{T}}_\mu])\\ &\quad\times \int_{-1}^1 dz\,\rho(z)\,\hat{\sigma}_{\Lambda_\Gamma}(k^2_{+K})\,, \end{aligned} \tag{6b}$$

where $\rho(z) = (3/4)(1-z^2)$, $k_{+K} = k + (z-1)K/2$; $\gamma^{\mathrm{T}}_\mu = T_{\mu\nu}(K)\gamma_\nu$, $f(k;K) = k\cdot K/(k^2K^2(k-K)^2)^{1/2}$; and $r_1 = 1/4$, $n_{0,1}$ are fixed by requiring that the zeroth Mellin moment of the leading-twist PDA of each diquark correlation is $[n\cdot K/n\cdot P]$, *i.e.* correctly normalised. The final elements are:

$$n\,\mathcal{S}(\ell;P) = i\int_{-1}^1 dz\,\rho(z)\,\hat{\sigma}_{\Lambda^0_p}(w_{+P})\,, \tag{7a}$$

$$\begin{aligned} n\,\mathcal{A}^j_\nu(\ell;P) &= r_{\mathcal{A}}\tfrac{1}{6} o^j \gamma_5[\gamma_\nu - i r_{\mathcal{P}} P_\nu]\\ &\quad\times \int_{-1}^1 dz\,\rho(z)\,\hat{\sigma}_{\Lambda^1_p}(w_{+P})\,, \end{aligned} \tag{7b}$$

where $w_{+P} = [-\ell_{+P} + (2/3)P]^2$; $o^+ = \sqrt{2}$, $o^0 = -1$; $r_{\mathcal{P}} = 13/87$; $r_{\mathcal{A}}$ measures the relative 1^+:0^+ diquark strengths in the Faddeev amplitude; and n is that amplitude's canonical normalisation constant, whose value ensures the proton has unit charge [32].

We choose the parameters in Eqs. (6), (7) so as to emulate realistic Faddeev wave functions [26,27,31,33]: $M = 2/5$, $M_0 = 2/3$,

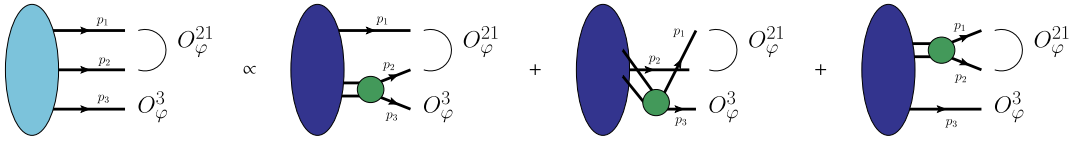

Fig. 2. Studies of the continuum three-body bound-state problem reveal that diquark correlations are an integral part of the proton's Poincaré-covariant wave function, Eqs. (3), (4). Hence, Eq. (1) is the sum of three terms, with the spinor projection operators given in Eq. (8). The (dark blue) ovals represent the $(\mathcal{S},\mathcal{A})$ elements in $\psi_{1,2,3}$, the (green) circles are the diquark correlation amplitudes, and the single and double lines are dressed-quark and -diquark propagators, respectively. (For interpretation of the colours in the figure(s), the reader is referred to the web version of this article.)

$M_1 = 3/4,\ \Lambda_\Gamma = 2/5,\ \Lambda_p^0 = 1,\ \Lambda_p^1 = 2/5$, in units of m_p,[1] with $r_{\mathcal{A}} = 0.30 \pm 0.03$ ensuring that the scalar diquark contribution to the proton's baryon number is $65 \pm 5\%$.

Eqs. (6), (7) define a constrained spectral function *Ansatz* for χ, whose fidelity will subsequently be tested. It delivers considerable simplification, *viz.* with algebraic representations that approximate numerical solutions of all equations relating to the proton bound state, our subsequent analysis is largely algebraic. Moreover, in addition to this simplicity, the character of our approach is quite general, being applicable to all cases in which one can use perturbation theory integral representations (PTIRs) for the propagators and amplitudes that arise in solving the continuum bound-state problem [34–36]. (This feature is again being exploited, *e.g.* Refs. [5,10, 37–42].) Hence, our subsequent algebraic analysis is realistic and also establishes an archetype for the continuum computation of baryon PDAs.

3. Proton PDA: calculation

Whenever the proton's Faddeev amplitude is as specified by Eqs. (3), (4), then Eq. (1) can be written as depicted in Fig. 2, where

$$\mathcal{O}^{21}_\varphi = H_- \, C^\dagger \not{n} \, H_+ , \ \ \mathcal{O}^3_\varphi = \not{n} \, H_+ . \tag{8}$$

As a concrete illustration, we consider the first diagram on the rhs, whose contribution to the proton's PDA is fully determined by the following Mellin moments:

$$i\tfrac{f_p}{2}\, n\cdot P \not{n}\, N_+ \int [dx]\, x_1^l x_2^m\, \varphi([x]) =: i\tfrac{f_p}{2}\, n\cdot P \not{n}\, N_+ \langle x_1^l x_2^m\rangle \tag{9a}$$

$$= \int [dx]\, x_1^l x_2^m \int \frac{d^4\ell}{(2\pi)^4}\frac{d^4k}{(2\pi)^4}\delta_n^{x_1}(\ell + P/3)\delta_n^{x_2}(k) \times \chi_1(\{p\},\{\alpha\},\{\sigma\})\, \mathcal{O}^{21}_\varphi\, \mathcal{O}^3_\varphi , \tag{9b}$$

where $\delta_n^x(p) = \delta(n\cdot p - x n\cdot P)$; $p_1 = \ell + P/3,\ p_2 = k,\ p_3 = K - k$.

Focusing on the proton's 0^+ diquark component, the second and third contributions in Fig. 2 vanish because this correlation is isoscalar-scalar. Hence the leading-twist part in Eq. (9b) is $\gamma\cdot\mathcal{L}^{0^+}$,

$$\mathcal{L}^{0^+}_\mu = \tfrac{1}{4}\mathrm{tr_D}\Big[S_d(p_3)\Gamma^0(k;K)\tilde{S}_u(p_2) H_- C^\dagger \not{n}\, H_+ \times S_u(p_1)\Delta^0(K)\mathcal{S}(\ell;P)\gamma_\mu \not{n}\, H_+\Big] \tag{10}$$

$$= \tfrac{1}{4}\mathrm{tr_D}\Big[\gamma_\mu \not{n}\, H_+ S_u(p_1)\Delta^0(K)\mathcal{S}(\ell;P)\Big] \times \tfrac{1}{2}\mathrm{tr_D}\Big[S_d(p_3)\Gamma^0(k;K)\tilde{S}_u(p_2) C^\dagger \not{n}\gamma_5\Big], \tag{11}$$

where we have used properties of $\mathrm{tr_D}$, the projection operators $H_\pm$, and n_μ. Inserting Eq. (11) into Eq. (9b), one finds unsurprisingly that the scalar diquark contribution to the proton's PDA is obtained from a convolution of the diquark's PDA with that of the bystander-quark in the quark+diquark Faddeev amplitude. The result generalises to the isotriplet-pseudovector component of the proton's wave function, in which case all three diagrams in Fig. 2 contribute to the proton's PDA.

Continuing our illustrative calculation, one first uses the methods described in Refs. [5,9] to compute all Mellin moments of the scalar diquark PDA, φ_0, which are derived from the second line of Eq. (11):

$$\mathcal{D}_0^m(K^2) = \frac{1}{P\cdot n}\int \frac{\mathrm{d}^4k}{(2\pi)^4}\left(\frac{k\cdot n}{P\cdot n}\right)^m \times \mathrm{tr_D}\Big[S_d(p_3)\Gamma^0(k,K)\tilde{S}_u(p_2)C^\dagger \not{n}\gamma_5\Big]. \tag{12}$$

Namely, in the k-integration of Eq. (12), use a Feynman parametrisation to rearrange the integrand such that there is a single denominator, a k-quadratic form raised to some power; and employ a suitably chosen change of variables in order to evaluate the integral over this relative four-momentum using standard algebraic methods. This yields, with $\bar{u} = 1-u$ and $z = -1 + 2[\bar{u}-\beta]/[\bar{u}-v]$,

$$\mathcal{D}_0^m(K^2) = n_0'(K^2)\left[\frac{n\cdot K}{n\cdot P}\right]^{1+m} \times \int \frac{du\,dv\,d\beta\,\beta^m\,\rho(z(u,v,\beta))2M}{[\beta(v[\beta-2]+\beta)+\bar{u}(v-\beta^2)][K^2+\mathcal{M}^2]}, \tag{13a}$$

$$\mathcal{M}^2 = \frac{[1-\bar{u}+v]M^2 + [\bar{u}-v]\Lambda_\Gamma^2}{\beta(v[\beta-2]+\beta)+\bar{u}(v-\beta^2)}[\bar{u}-v]. \tag{13b}$$

In our case, one can straightforwardly obtain the following algebraic result when $\Lambda_\Gamma = M$ ($\hat{x}_3 = 1-\hat{x}_2,\ \hat{x}_2 = x_2/[x_2+x_3]$, $y = M^2/K^2$):

$$n_0''(K^2)\,\varphi_0(\hat{x}_2,\hat{x}_3) = 12 y\Big(1 - \frac{y}{\hat{x}_2\hat{x}_3}\ln[1+\hat{x}_2\hat{x}_3/y]\Big), \tag{14}$$

where $n_0''(K^2)$ ensures $1 = \int dx \varphi_0(x,1-x)$ at each K^2. Notably, consistent with expectations and detailed calculations [5,43], when $K^2 \ll \Lambda_\Gamma^2$, $\varphi_0(\hat{x}_2,\hat{x}_3) = 6\hat{x}_2\hat{x}_3$, *viz.* the two-body conformal-limit PDA, which describes a correlation-free system; whereas on $K^2 \gg \Lambda_\Gamma^2$, $\varphi_0(\hat{x}_2,\hat{x}_3) = 1$, which is the PDA of a pointlike two-body composite, the most highly-correlated system possible.

Using Eqs. (13), suppressing n in Eq. (7), one can rewrite Eq. (9b) in the form ($p_1 = \ell + P/3,\ K = -p_1 + P$):

$$i\tfrac{f_p}{2}\,[n\cdot P]^2 \not{n}\langle x_1^l x_2^m\rangle = \int \frac{d^4\ell}{(2\pi)^4}\left[\frac{n\cdot p_1}{n\cdot P}\right]^l \times \tfrac{1}{4}\gamma^\mu \mathrm{tr_D}\Big[\gamma_\mu \not{n}\, H_+ S_u(p_1)\Delta^0(K)\mathcal{S}(\ell;P)\Big]\mathcal{D}_0^m(K^2), \tag{15}$$

[1] The ordering of masses is determined by extant analyses; and their values and those of the widths are fixed through comparisons with numerical solutions of the Faddeev equation. We use simple fractions to highlight that the values are approximate. Nevertheless, our PDA results are qualitatively insensitive to character-preserving variations in these values; and the quantitative comparisons are not markedly affected by 10% variations.

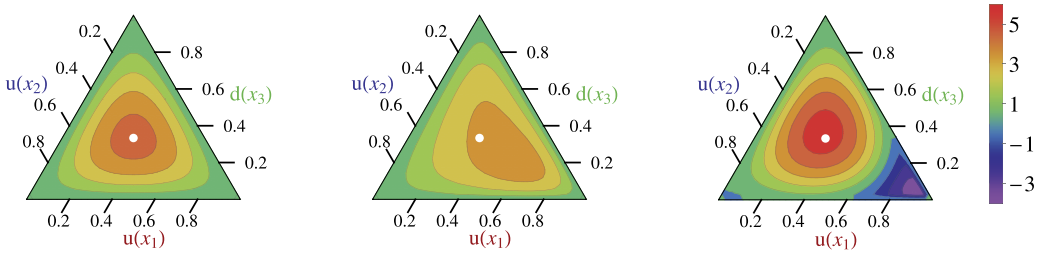

Fig. 3. Barycentric plots: *left panel* – conformal limit PDA, $\varphi_N^{\rm cl}([x]) = 120 x_1 x_2 x_3$; *middle panel* – computed proton PDA evolved to $\zeta = 2$ GeV, which peaks at $([x]) = (0.55, 0.23, 0.22)$; and *right panel* – Roper resonance PDA at $\zeta = 2$ GeV. The white circle in each panel serves only to mark the centre of mass for the conformal PDA, whose peak lies at $([x]) = (1/3, 1/3, 1/3)$.

at which point the analysis leading to Eqs. (13) can be adapted to solve this final "two-body" (quark+diquark) convolution problem for the 0^+-diquark component of $\varphi([x];\zeta)$. Namely, using a carefully chosen redefinition of Feynman parameters, as done to reach Eqs. (13) from Eq. (12), and making the change of variables $\beta \to (1-\alpha)\beta$, with $0 < \alpha < 1$, one finds

$$\langle x_1^l x_2^m \rangle = \int_0^1 d\alpha\, \alpha^l \int_0^{1-\alpha} d\beta\, \beta^m f(\alpha,\beta)\,, \tag{16}$$

where the function $f(\alpha,\beta)$ is an integral over five Feynman parameters in which the denominator is a single ℓ-quadratic form. Given this structure, one immediately identifies $f(x_1 = \alpha, x_2 = \beta)$ as the scalar diquark contribution to the proton PDA.

The complete result for $\varphi([x];\zeta)$ is obtained by adding the 1^+-diquark contributions. That is readily accomplished by employing the procedure sketched above. The addition is a sum of three integrals, two involving seven Feynman parameters, the third, nine, and each with a denominator that is an ℓ-quadratic form. This verbal description is simple; and, albeit lengthy, so are the final expressions.

All integrals required to compute $\varphi([x];\zeta)$ are easily evaluated numerically. The distribution thus obtained is that associated with the hadronic scale $\zeta = \zeta_H = 0.5$ GeV [44]. We evolve $\varphi([x];\zeta_H)$ to $\zeta = \zeta_2 = 2$ GeV by adapting the algorithm in Refs. [5,6] to the case of baryons, *i.e.* generalising the functional representation in Ref. [45] and using the leading-order evolution equation in Ref. [3]. The result is depicted in Fig. 3 and efficiently interpolated using $(w_{00} = 1)$

$$\varphi([x]) = n_\varphi\, x_1^{\alpha_-} (x_2 x_3)^{\beta_-} \sum_{j=0}^{2} \sum_{i=0}^{j} w_{ij}\, P_{j-i}^{2[i+\beta];\alpha_-}(2x_1 - 1) \times (x_2 + x_3)^i C_i^\beta([x_3 - x_2]/[x_2 + x_3])\,, \tag{17}$$

where n_φ ensures $\int [dx] \varphi([x]) = 1$; $(\alpha,\beta)_- = (\alpha,\beta) - 1/2$; P is a Jacobi function, C a Gegenbauer polynomial; and the interpolation parameters are listed in Table 1A.

Table 1B lists the four lowest-order moments of our proton PDA. They reveal valuable insights, *e.g.* when the proton is drawn as solely a quark+scalar-diquark correlation, $\langle x_2 \rangle_u = \langle x_3 \rangle_d$, because these are the two participants of the scalar quark+quark correlation; and the system is very skewed, with the PDA's peak being shifted markedly in favour of $\langle x_1 \rangle_u > \langle x_2 \rangle_u$. This outcome conflicts with lQCD results [16,17].

On the other hand, as noted above, it is a longstanding prediction of Faddeev equation calculations that pseudovector diquark correlations are an essential part of the proton's wave function, *e.g.* Refs. [46–49]. Naturally, when these $\{uu\}$ and $\{ud\}$ correlations are included, momentum is shared more evenly, shifting from the bystander $u(x_1)$ quark into $u(x_2)$, $d(x_3)$. Adding these correlations with the known weighting, the PDA's peak moves back toward the centre and our computed values of the first moments align with those obtained using lQCD. As evident from the table, this result is quantitatively insensitive to realistic variations in the strength of the 1^+-diquark component. Consequently, the confluence delivers a more complete understanding of the lQCD simulations, which are now seen to confirm the picture of a proton as a bound-state with both strong scalar *and* pseudovector diquark correlations, in which the scalar diquarks are responsible for $\approx 60\%$ of the Faddeev amplitude's canonical normalisation. Importantly, as found with ground-state S-wave mesons [5–8,10,11], the leading-twist PDA of the ground-state nucleon is both broader than $\varphi_N^{\rm cl}([x])$ and decreases monotonically away from its maximum in all directions.

Table 1
A – Eq. (17) interpolation parameters for the proton and Roper PDAs in Fig. 3. *B* – Computed values of the first four moments of the PDAs. f_N is listed in units of 10^{-3} GeV^2, and our error reflects a scalar diquark content of $65 \pm 5\%$. Values in rows marked with "$\not\supset$ av" were obtained assuming the baryon is constituted solely from a scalar diquark. (All results listed at $\zeta = 2$ GeV.)

A	$n_{\hat\varphi}$	α	β	w_{01}	w_{11}	w_{02}	w_{12}	w_{22}
p	65.8	1.47	1.28	0.096	0.094	0.15	−0.053	0.11
R	14.4	1.42	0.78	−0.93	0.22	−0.21	−0.057	−1.24

B	f_N	$\langle x_1 \rangle_u$	$\langle x_2 \rangle_u$	$\langle x_3 \rangle_d$
conformal PDA		0.333	0.333	0.333
lQCD [16]	2.84(33)	0.372(7)	0.314(3)	0.314(7)
lQCD [17]	3.60(6)	0.358(6)	0.319(4)	0.323(6)
herein proton	3.78(14)	0.379(4)	0.302(1)	0.319(3)
herein proton $\not\supset$ av	2.97	0.412	0.295	0.293
herein Roper	5.17(32)	0.245(13)	0.363(6)	0.392(6)
herein Roper $\not\supset$ av	2.63	0.010	0.490	0.500

4. Roper PDA

Our framework is readily extended to describe the quark core of the proton's first radial excitation: $m_R = (3/2) m_p$ [27,31]. The scalar functions in this system's Faddeev amplitude possess a zero at quark–diquark relative momentum $\sqrt{\ell^2} \approx 0.4$ GeV $\approx 1/[0.5$ fm$]$, a property that can be expressed in our algebraic amplitude by modifying the spectral functions in Eqs. (7) following the pattern:

$$\rho(z) = (1 - z^2) \to \rho_R(z) = s_R^{qq}(1 - z^2)(z + z_R^{qq})\,, \tag{18}$$

where (s_R^{qq}, z_R^{qq}) are parameters. Requiring that the amplitude obtained therewith is consistent with known Faddeev equation solutions for the first radial excitation, one obtains $(s_R^S, z_R^S) = (-1, 1/50) = (s_R^{\mathcal{A},\gamma}, z_R^{\mathcal{A},\gamma})$, $(s_R^{\mathcal{A},P}, z_R^{\mathcal{A},P}) = (1, 3/10)$ and, in Eq. (7a), $\Lambda_p^0 \to \Lambda_R^0 = 4/5$.

This procedure yields the PDA in the rightmost panel of Fig. 3, which is efficiently interpolated using Eq. (17) with the parameters in Table 1A; and whose first four moments are listed in Table 1B. The prediction reveals some curious features, *e.g.*: the excitation's PDA is not positive definite and there is a locus of zeros in the lower-right corner of the barycentric plot, both of which echo features of the wave function for the first radial excitation of a quantum mechanical system and have also been seen in the leading-twist PDAs of radially excited mesons [50,51]; and the impact of pseudovector correlations within this excitation is opposite to that in the ground-state, *viz.* they shift momentum into $u(x_1)$ from $u(x_2)$, $d(x_3)$.

5. Epilogue

Using perturbation theory integral representations (PTIRs) for the proton and Roper resonance Faddeev wave functions, constrained by available solutions of the continuum three-valence-body bound-state equations, we delivered a quantum field theory calculation of the pointwise behaviour of the PDAs of these systems, revealing novel features, *e.g.* the ground state's PDA is a broad, concave function of its arguments whose structural features reveal the presence of large pseudovector diquark components in the proton's wave function via comparison with lattice-QCD analyses of its lowest-order moments; and the radial excitation's PDA exhibits a locus of zeros.

The general character of our approach is also worth highlighting: it can be used with any Poincaré-covariant bound-state wave function for which a PTIR exists. Hence, whilst our PDA predictions may be called sketches, owing to the deliberate simplicity of our analysis, their veracity can straightforwardly be tested in future studies. Moreover, they can readily be improved; but given the robust nature of the constraints we have employed, such improvements will not qualitatively change the character of these PDAs, and any quantitative changes will be modest. It follows that the PDAs we have determined will, *e.g.* enable realistic assessments to be made of the scale at which exclusive experiments involving baryons may properly be compared with predictions based on perturbative-QCD hard scattering formulae and thereby assist existing and planned facilities to reach their full potential. The value of such estimates has recently been demonstrated in studies of mesons [8,40].

Acknowledgements

We are grateful for insightful comments from V. Mokeev, H. Moutarde, F. Gao, S.-X. Qin, J. Rodríguez-Quintero and S.-S. Xu. Work supported by: Argonne National Laboratory, Office of the Director's Postdoctoral Fellowship Program; European Union's Horizon 2020 research and innovation programme under the Marie Skłodowska-Curie Grant Agreement No. 665919; Spanish MINECO's Juan de la Cierva-Incorporación programme, Grant Agreement No. IJCI-2016-30028; Spanish Ministerio de Economía, Industria y Competitividad under Contract Nos. FPA2014-55613-P and SEV-2016-0588; the Chinese Government's Thousand Talents Plan for Young Professionals; the Chinese Ministry of Education, under the *International Distinguished Professor* programme; and U.S. Department of Energy, Office of Science, Office of Nuclear Physics, under contract no. DE-AC02-06CH11357.

References

[1] B.D. Keister, W.N. Polyzou, Adv. Nucl. Phys. 20 (1991) 225–479.
[2] S.J. Brodsky, H.-C. Pauli, S.S. Pinsky, Phys. Rep. 301 (1998) 299–486.
[3] G.P. Lepage, S.J. Brodsky, Phys. Rev. D 22 (1980) 2157–2198.
[4] S.J. Brodsky, G.F. de Teramond, Phys. Rev. Lett. 96 (2006) 201601.
[5] L. Chang, I.C. Cloët, J.J. Cobos-Martinez, C.D. Roberts, S.M. Schmidt, P.C. Tandy, Phys. Rev. Lett. 110 (2013) 132001.
[6] C. Shi, C. Chen, L. Chang, C.D. Roberts, S.M. Schmidt, H.-S. Zong, Phys. Rev. D 92 (2015) 014035.
[7] V.M. Braun, S. Collins, M. Göckeler, P. Pérez-Rubio, A. Schäfer, R.W. Schiel, A. Sternbeck, Phys. Rev. D 92 (2015) 014504.
[8] T. Horn, C.D. Roberts, J. Phys. G 43 (2016) 073001.
[9] C. Mezrag, H. Moutarde, J. Rodríguez-Quintero, Few-Body Syst. 57 (2016) 729–772.
[10] F. Gao, L. Chang, Y.-X. Liu, Phys. Lett. B 770 (2017) 551–555.
[11] J.-H. Zhang, J.-W. Chen, X. Ji, L. Jin, H.-W. Lin, Phys. Rev. D 95 (2017) 094514.
[12] J.-W. Chen, L. Jin, H.-W. Lin, A. Schäfer, P. Sun, Y.-B. Yang, J.-H. Zhang, R. Zhang, Y. Zhao, Kaon distribution amplitude from lattice QCD and the flavor SU(3) symmetry, arXiv:1712.10025 [hep-ph].
[13] V.L. Chernyak, A.R. Zhitnitsky, Phys. Rep. 112 (1984) 173.
[14] N.G. Stefanis, M. Bergmann, Phys. Rev. D 47 (1993) R3685–R3689.
[15] V.M. Braun, et al., Phys. Rev. D 79 (2009) 034504.
[16] V.M. Braun, S. Collins, B. Gläßle, M. Göckeler, A. Schäfer, R.W. Schiel, W. Söldner, A. Sternbeck, P. Wein, Phys. Rev. D 89 (2014) 094511.
[17] G.S. Bali, et al., J. High Energy Phys. 02 (2016) 070.
[18] V. Braun, R.J. Fries, N. Mahnke, E. Stein, Nucl. Phys. B 589 (2000) 381–409; Erratum: Nucl. Phys. B 607 (2001) 433.
[19] R.T. Cahill, C.D. Roberts, J. Praschifka, Aust. J. Phys. 42 (1989) 129–145.
[20] C.J. Burden, R.T. Cahill, J. Praschifka, Aust. J. Phys. 42 (1989) 147–159.
[21] R.T. Cahill, Aust. J. Phys. 42 (1989) 171–186.
[22] H. Reinhardt, Phys. Lett. B 244 (1990) 316–326.
[23] G.V. Efimov, M.A. Ivanov, V.E. Lyubovitskij, Z. Phys. C 47 (1990) 583–594.
[24] J. Segovia, C.D. Roberts, S.M. Schmidt, Phys. Lett. B 750 (2015) 100–106.
[25] D. Binosi, C. Mezrag, J. Papavassiliou, C.D. Roberts, J. Rodríguez-Quintero, Phys. Rev. D 96 (2017) 054026.
[26] J. Segovia, I.C. Cloët, C.D. Roberts, S.M. Schmidt, Few-Body Syst. 55 (2014) 1185–1222.
[27] J. Segovia, B. El-Bennich, E. Rojas, I.C. Cloët, C.D. Roberts, S.-S. Xu, H.-S. Zong, Phys. Rev. Lett. 115 (2015) 171801.
[28] S.-S. Xu, C. Chen, I.C. Cloët, C.D. Roberts, J. Segovia, H.-S. Zong, Phys. Rev. D 92 (2015) 114034.
[29] G. Eichmann, C.S. Fischer, H. Sanchis-Alepuz, Phys. Rev. D 94 (2016) 094033.
[30] Y. Lu, C. Chen, C.D. Roberts, J. Segovia, S.-S. Xu, H.-S. Zong, Phys. Rev. C 96 (2017) 015208.
[31] C. Chen, B. El-Bennich, C.D. Roberts, S.M. Schmidt, J. Segovia, S. Wan, Phys. Rev. D 97 (2018) 034016.
[32] M. Oettel, M. Pichowsky, L. von Smekal, Eur. Phys. J. A 8 (2000) 251–281.
[33] J. Segovia, C.D. Roberts, Phys. Rev. C 94 (2016), 042201(R).
[34] N. Nakanishi, Phys. Rev. 130 (1963) 1230–1235.
[35] N. Nakanishi, Prog. Theor. Phys. Suppl. 43 (1969) 1–81.
[36] N. Nakanishi, Graph Theory and Feynman Integrals, Gordon and Breach, New York, 1971.
[37] S.M. Dorkin, L.P. Kaptari, B. Kämpfer, Phys. Rev. C 91 (2015) 055201.
[38] K. Raya, M. Ding, A. Bashir, L. Chang, C.D. Roberts, Phys. Rev. D 95 (2017) 074014.
[39] J. Carbonell, T. Frederico, V.A. Karmanov, Eur. Phys. J. C 77 (2017) 58.
[40] F. Gao, L. Chang, Y.-X. Liu, C.D. Roberts, P.C. Tandy, Phys. Rev. D 96 (2017) 034024.
[41] W. de Paula, T. Frederico, G. Salmè, M. Viviani, R. Pimentel, Eur. Phys. J. C 77 (2017) 764.
[42] N. Chouika, C. Mezrag, H. Moutarde, J. Rodríguez-Quintero, Phys. Lett. B 780 (2018) 287–293.
[43] S.-X. Qin, C. Chen, C. Mezrag, C.D. Roberts, Phys. Rev. C 97 (2018) 015203.
[44] C. Chen, L. Chang, C.D. Roberts, S. Wan, H.-S. Zong, Phys. Rev. D 93 (2016) 074021.
[45] V.M. Braun, S.E. Derkachov, G.P. Korchemsky, A.N. Manashov, Nucl. Phys. B 553 (1999) 355–426.
[46] N. Ishii, W. Bentz, K. Yazaki, Phys. Lett. B 318 (1993) 26–31.
[47] N. Ishii, W. Bentz, K. Yazaki, Nucl. Phys. A 587 (1995) 617–656.
[48] V. Keiner, Z. Phys. A 359 (1997) 91–97.
[49] M. Oettel, G. Hellstern, R. Alkofer, H. Reinhardt, Phys. Rev. C 58 (1998) 2459–2477.
[50] B.L. Li, L. Chang, F. Gao, C.D. Roberts, S.M. Schmidt, H.S. Zong, Phys. Rev. D 93 (2016) 114033.
[51] B.-L. Li, L. Chang, M. Ding, C.D. Roberts, H.-S. Zong, Phys. Rev. D 94 (2016) 094014.